

Military Technical College
Kobry El-Kobbah,
Cairo, Egypt



8th International Conference
on Civil and Architecture
Engineering
ICCAE-8-2010

**Effects of friction damper-brace design parameters
on seismic performance of multistory building structures**

By

Hamid Masaeli*

Abstract:

In this study, design parameters of friction damper-brace system (FDBS) and their influence on seismic response of low-to-medium-rise building structures are investigated and a guide for optimal design procedure of FDBS is presented. First, numerical dynamic model of a SDOF building structure equipped with FDBS is proposed. Then, design parameters of FDBS in SDOF structures are introduced and their influence on dynamic response of the system is examined. Next, the numerical dynamic model and design parameters of FDBS are generalized to MDOF building structures. In this stage, numerical analyses were performed on some example building models and improvement of seismic response of the structures with respect to variations of design parameters of FDBS including: total slip-load ratio of friction damper devices (FDD), number of FDD installations, and arrangement of dampers along height of building structures, was investigated. In order to evaluate effects of fundamental period of the structure on design procedure of the FDBS, different periods were considered. To examine arrangements of FDD installations along height of the structures, different states of damper placement were compared.

Keywords:

Passive structural control, friction damper, optimal design, seismic performance, and multistory building structures.

* Department of Civil Engineering, Sharif University of Technology, Tehran, Iran.

1. Introduction:

Many researches have been accomplished by now on seismic response reduction of building structures using friction dampers. Because this passive structural controlling system, with its frictional hysteretic behavior, is capable to dissipate a large amount of seismic input energy.

Several types of friction damper devices have been presented with similar energy dissipation mechanisms. Pall and Marsh proposed a friction damper installed at the crossing joint of the X-brace to avoid the compression in the brace member [1]. Constantinou *et al.* proposed a friction damper composed of a sliding steel shaft and two friction pads clamped by adjustable bolts [2]. Grigorian *et al.* examined the energy dissipation effect of a joint with slotted bolt holes [3]. Mualla and Belev proposed a rotational friction damper with adjustable slip-moment [4]. In addition, Dyke *et al.* presented a novel magneto-rheological (MR) fluid damper that has the characteristics of friction damping [5].

There have been several experimental and analytical studies on seismic performance of multistory building structures and effects of friction dampers on mitigating structural responses have been investigated. Aiken *et al.* examined seismic response of a nine-storey steel frame with friction damped cross-bracing [6–11]. On the other hand, in the design of energy dissipation passive devices for seismic structural control, it is the most important factor to determine design parameters systematically. To restate, the topological distribution and size of these devices must be designed in accordance with a systematic and well-established design methodology in order to achieve a desired structural performance under a specified seismic environment. However, the lack of such design methodology has conducted many examples of studies on optimal design of energy dissipative devices during last decade [12–21]. Within these researches, Garcia and Soong proposed a simplified sequential search algorithm (SSSA), which gives optimal floor distribution of the viscous damping by repeated installation of unit viscous dampers on the floor with the largest controllability index defined by inter-storey drift or relative velocity. That procedure was imposed on a series of example MDOF structures typically and efficiency of the methodology was evaluated [22]. On the other hand, Lee *et al.* investigated design parameters of friction damper brace system, including allocation and slip load of friction dampers. For this purpose, numerical analyses were performed on a number of example structures (previously used by Garcia and Soong [22]) with short fundamental natural periods. Results of numerical analyses led to an empirical equation on the optimal number of friction damper installations. But it must be noted that since only short-period structures were used in numerical analyses, the conclusions of that study are valid only for building structures with short fundamental natural periods [23].

The purpose of this study is to investigate the effects of design parameters of friction

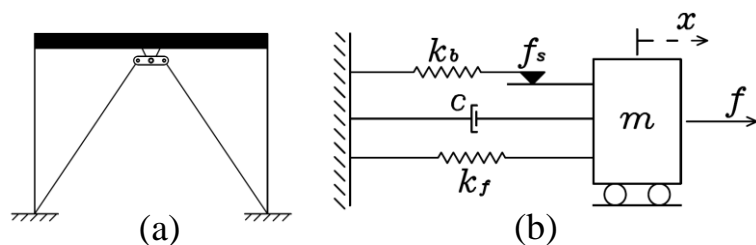
damper-brace system (FDBS) on seismic performance of multistory, low-to-medium-rise building structures with different fundamental natural periods. First, seismic responses of SDOF structures with respect to variations of FDBS design parameters, including stiffness and slip-load ratios, are evaluated. Second, results of a large number of numerical analyses on MDOF building structures equipped with FDBS are presented to investigate performance of the structures with respect to variations of generalized FDBS design parameters, including total slip-load ratio, number of friction damper device (FDD) installations, and FDD arrangement along height of the structure. Finally, considering results obtained from numerical analyses, a guide for design procedure of FDBS is proposed.

2. Dynamic model of friction damper-brace system (FDBS):

2.1. FDBS in SDOF structures:

A SDOF structure equipped with FDBS is presented in Figure (1)–a. It consists a shear single-storey frame, a chevron brace, and a rotational friction damper device (proposed by Mualla and Belev [5]) on midspan of the grider. Figure (1)–b represents a basic dynamic model of the original system, where k_f , m , and c denote the lateral stiffness, mass, and damping of the frame, and k_b , f_s , x , and f denote the lateral stiffness of the brace, the slip-load of the friction damper, the displacement of the frame, and the external load, respectively.

Figure (1): (a) A SDOF structure equipped with FDBS; (b) Dynamic model of the original system.



Dynamic behavior of the model during seismic excitations can be described in the two following stages:

- *Stage 1: Stick stage.* Internal force of the friction damper device (FDD) is less than slip-load (f_s) and consequently no rotation is observed in FDD. In this stage, friction damper brace system (FDBS) is similar to a chevron brace.
- *Stage 2: Slip stage.* Internal force of the FDD is equal to f_s and consequently the FDD yields. Lateral stiffness of the FDD is negligible in this condition. The sliding stage endures while the internal force remains equal to f_s .

Accordingly, the FDD is assumed to have rigid-perfectly-plastic behavior. On the other hand, the primary structure and the brace are assumed to behave elastically. Therefore, the force-displacement relation of a system equipped with the FDBS can be modeled as a bilinear behavior as presented in Figure (2). As shown, $(k_f + k_b)$ is primary linear-

elastic stiffness; k_f is secondary strain hardening stiffness of the system; and f_y denotes equivalent yield strength which can be represented by the following equation [24].

$$f_y = f_s \left(\frac{k_f + k_b}{k_b} \right) \tag{1}$$

In this study, the numerical analyses were performed using well-known Newmark- β method (assuming: $\beta=1/6$ and $\gamma=1/2$) [25] for simulating the dynamic responses of bilinear systems.

In order to verify the proposed numerical method, a single-storey steel frame equipped with FDBS which Mualla and Belev [5] had experimentally investigated, was modeled. Figure (3)–a (dark color curve) shows time history of displacement in the structure under El Centro NS ground motion presented by Mualla and Belev [5]. Figure (3)–b presents the same response in the proposed model which shows a good accuracy and agreement with experimental results. Bilinear hysteretic behavior of the model is shown in Figure (4), in which summation of hysteresis loops areas represents total energy dissipated by frictional behavior of the FDBS.

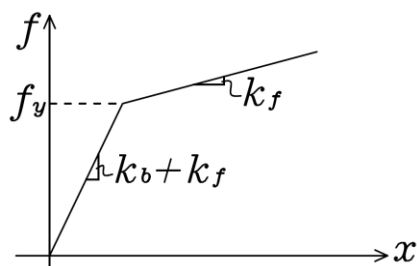


Figure (2): Bilinear force-displacement relation of a SDOF system equipped with FDBS.

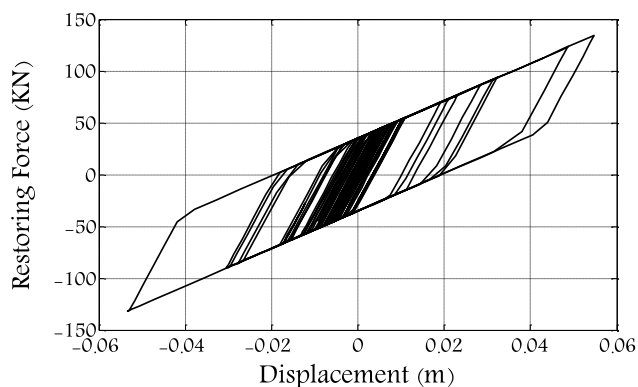


Figure (4): Bilinear hysteretic behavior of the proposed model under El Centro NS ground motion.

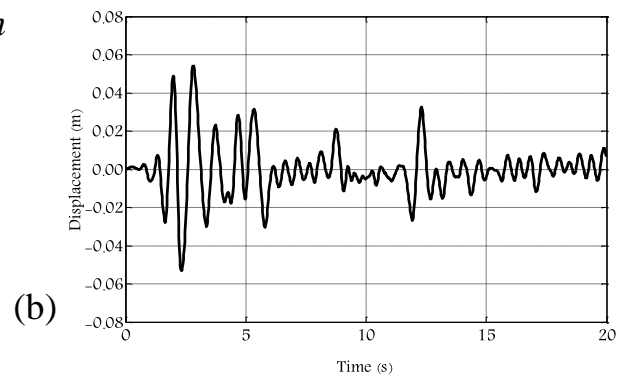
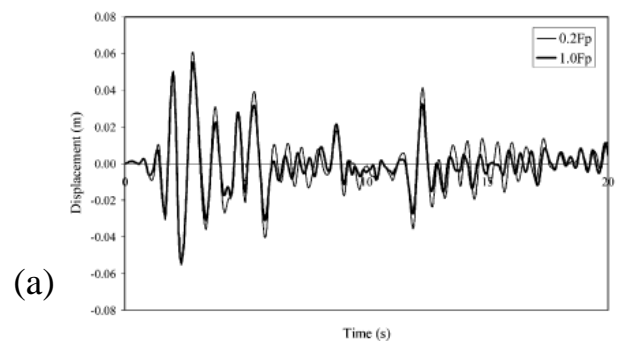


Figure (3): (a) Time history of displacement in a single-storey steel frame under El Centro NS ground motion presented by Mualla and Belev [5] (dark color curve); (b) Time history of displacement in proposed model.

2.1. Generalization to MDOF building structures:

When FDBS is installed on MDOF building structures, each FDD has an independent bilinear hysteretic behavior under seismic loading. Therefore, the whole system has a nonlinear dynamic response that can be modeled with generalizing the previous proposed numerical method. For this purpose, stick or slip phase of each FDD is separately controlled during each time step of dynamic analysis.

3. Design parameters of FDBS:

3.1. Design for SDOF structures:

3.1.1. FDBS design parameters formulation:

According to Figure (2), the bilinear force-displacement relation of the SDOF system depends on two design parameters of the FDBS.

The first design parameter is stiffness of the brace (k_b) that can be normalized by stiffness of the frame (k_f). The obtained stiffness ratio (SR) is expressed as follows:

$$SR = \frac{k_b}{k_f} \quad (2)$$

The second design parameter is slip-load of the FDD (f_s) that can be normalized by storey weight (W) of the SDOF system, as follows:

$$\rho = \frac{f_s}{W} \quad (3)$$

where ρ is normalized slip-load of the FDD.

3.1.2. Performance index:

For linear structures, where the structure does not suffer structural damage, the peak inter-story drift becomes an important response parameter, since it is a measure of nonstructural damage [16]. Therefore, peak inter-storey drift is considered as performance index of the structure in this study and is assumed to be normalized by peak inter-storey drift of the bare frame [23], as follows:

$$R_d = \frac{|x_i(t)|_{\max}}{|x_{0,i}(t)|_{\max}} \quad (5)$$

where R_d , $x(t)$, and $x_0(t)$ are relative peak inter-storey drift and time history of inter-storey drift in equipped and bare frame, respectively.

3.1.3. Effects of FDBS design parameters on response of SDOF structures:

Results of numerical analyses are presented in order to investigate the effects of design parameters of the FDBS on performance of SDOF structures. Figure (5) and (6) show variations of performance index (R_d) versus design parameters of SR and ρ , respectively,

for a SDOF system with different fundamental periods of the primary structure equal to 0.1 s through 0.5 s, and damping ratio equal to 0.02, under El Centro ground motion typically. In Figure (5) in which ρ is assumed equal to 0.25, R_d decreases when the first design parameter, SR , increases. As shown, R_d decreases rapidly as SR increases in the range of $0 < SR < 5$, so that response reduction is equal to or greater than about 80% when SR is set equal to 5. On the other hand, in Figure (6) in which SR is assumed equal to 5, R_d has a primary decrease when ρ increases and then remains constant after a particular value of ρ . This fact shows that if slip-load ratio of the FDD is greater than a particular value, seismic loading cannot activate the FDD and then no slip stage occurs during earthquake. In such condition, the FDBS behaves like an ordinary chevron brace.

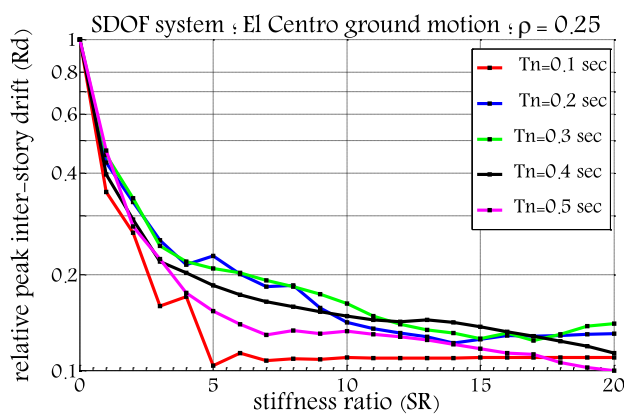


Figure 5. Variations of performance index (R_d) versus stiffness ratio (SR) of the brace in a SDOF system.

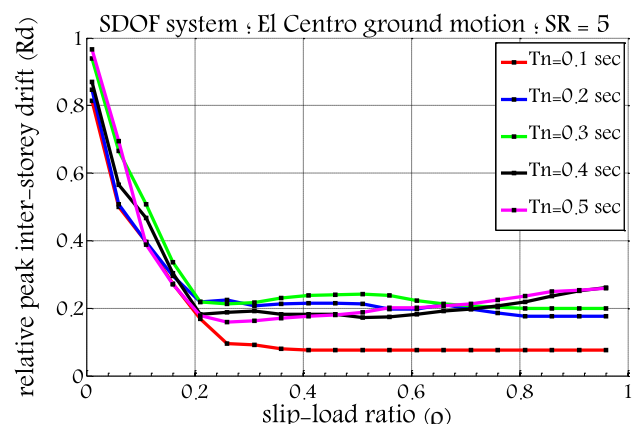


Figure 6. Variations of performance index (R_d) versus slip-load ratio (ρ) of the FDD in a SDOF system.

3.2. Design for MDOF building structures:

3.2.1. FDBS design parameters formulation:

In generalization to MDOF building structures, four design parameters can be defined. The first design parameter is stiffness ratio (SR) of each FDBS as follows:

$$SR_i = \frac{k_{bi}}{k_{fi}} \tag{6}$$

where SR_i is stiffness ratio of FDBS which is installed on i -th floor of the MDOF building structure. In addition, k_{bi} and k_{fi} are stiffness of i -th FDBS and lateral stiffness of i -th floor, respectively.

The second design parameter is number of FDD's which are installed on different stories of the MDOF building structure. Number of FDD installations is denoted by N_f in this paper.

The third design parameter is total slip-load ratio (ρ) of all FDD's installed on the MDOF building structure that is expressed by the following equation:

$$\rho = \frac{\sum_{i=1}^{N_f} f_{si}}{\sum_{i=1}^N W_i} \quad (7)$$

where ρ is total slip-load ratio of all installed FDD's and f_{si} , W_i , N_f , and N denote slip-load of i -th FDD, weight of i -th storey, number of FDD installations, and number of stories, respectively. This total slip-load ratio must be distributed amongst FDD's and then indicates normalized slip-load of each FDD. In this study, total slip-load ratio is distributed amongst FDD's identically.

The last FDBS design parameter is arrangement of FDD's along height of the MDOF building structure. This parameter indicates which stories are chosen and equipped for any arbitrary N_f .

3.2.2. Performance index:

Performance index in MDOF building structures is a generalized form of Eq. (5) as expressed by the following equation:

$$R_d = \frac{\max_{i=1, \dots, N} \{ |x_i(t)|_{\max} \}}{\max_{i=1, \dots, N} \{ |x_{0,i}(t)|_{\max} \}} \quad (8)$$

where R_d , $x_i(t)$, and $x_{0,i}(t)$ are relative peak inter-storey drift and time history of i -th inter-storey drift before and after damper installation, respectively, and N is total number of stories.

4. Effects of FDBS design parameters on response of MDOF building structures:

Numerical analyses show that performance of MDOF building structures, equipped with FDBS, changes with respect to variations of: 1) structural properties; 2) seismic loading; and 3) FDBS design parameters, with considerable nonlinearity. Therefore, in order to investigate effects of the FDBS design parameters on improvement of structural performance, numerous example building structures are investigated in this study, considering variations in dynamic characteristics, input earthquake ground motions, and FDBS design parameters.

4.1. Description of example building structures and ground motions:

In this study, building structures with five different numbers of stories are considered: 4, 6, 8, 10, and 12, which represent low-to-medium-rise buildings. The corresponding stiffness properties are summarized in Table 1, where it can be seen that the stiffness at a given storey is always equal to either 100% or 85% of the stiffness at the storey below. Therefore, conclusions of this study are valid only for building structures with no

stiffness irregularities. For each number of stories, five fundamental natural periods are considered. The total number of building models constructed is then 25. For a given model, all the storey masses are equal. Mass properties corresponding to different fundamental natural periods are summarized in Table 2. The inherent damping ratio ξ_0 of the structural models is in all cases equal to 2% for all modes and Rayleigh damping matrix is considered [25].

For the purpose of investigating input earthquake ground motion effects on FDBS design, three recorded seismic ground motions: El Centro 1940, Northridge 1994, and Loma Prieta 1989 are used to perform the numerical analyses.

Table (1): Stiffness properties of the building models

Storey	Storey stiffness (kN/cm)				
	Number of stories in building models				
	4	6	8	10	12
1 - 2	1000	1000	1000	1000	1000
3 - 4	1000	1000	1000	1000	1000
5 - 6		850	850	850	850
7 - 8			850	850	850
9 - 10				725	725
11 - 12					725

Table (2): Mass properties of the building models

MDOF Structure	Fundamental Period (sec)	Storey Mass (kg)
4-storey	0.8	195 530
	1.0	305 500
	1.2	439 950
6-storey	1.4	598 800
	1.0	133 620
	1.2	192 420
8-storey	1.4	261 900
	1.6	342 080
	1.2	108 990
10-storey	1.4	148 330
	1.6	193 750
	1.8	245 200
12-storey	1.4	90 000
	1.6	117 550
	1.8	148 780
12-storey	2.0	183 680
	1.6	79 600
	1.8	100 740
12-storey	2.0	124 380
	2.2	150 500

4.2. FDBS design assumptions in numerical analyses:

In accordance with what was stated before, there are four design parameters that must be determined so that the best efficiency would be obtained for the FDBS. The first design parameter SR_i , as defined in Eq. (6), is set equal to 5 for all FDD's during all

numerical analyses, with regard to Figure (5) This figure shows that application of braces with higher stiffness does not decrease response of the SDOF structure significantly. This fact is also observed in MDOF building structures.

Results of a study presented by Lee *et al.* [23] on slip-load and allocation of FDD's in MDOF building structures, show that optimal number of FDD installations (N_f) is almost half of total number of stories (N) in short-period building structures. On the other hand, fundamental natural periods of example structures in this study, as shown in Table 2, are generally more than assumed periods of Lee *et al.* (i.e. the example structures presented in this study have less stiffness). Therefore, for a given N -storey building structure with periods shown in Table 2, the expected optimal value of normalized number of FDD installations (N_f/N) must be in the range of 0.5 through 1. Consequently, variations of the second FDBS design parameter during numerical analyses are corresponding to range of $0.5 \leq (N_f/N) \leq 1$.

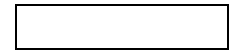
Total slip-load ratio of FDD's (ρ), as defined in Eq. (7), is assumed to vary in the range of 0.1 through 2. Results of numerical analyses show that optimal value of ρ , as the third FDBS design parameter, occurs within this range. In addition, all states of FDD's arrangement along height of the building structure, as the forth FDBS design parameter, are considered during numerical analyses and the best configurations are explored.

5. Results and discussion:

Numerical analyses were performed with respect to assumptions stipulated in previous section. Variations of FDBS design parameters produce numerous states of problems which were solved and optimal values of FDBS design parameters were explored minimizing performance index of the structures. Table 3 contains optimal states of the FDBS design parameters obtained from the numerical analyses. In addition, efficiency of the FDBS in mitigation of dynamic response of the building models is evaluated between 40 through 85 percents in accordance with the results of Table 3.

Table (3): Summary results of numerical analyses

Earthquake	Structure	Fundamental Period (sec)	Total Slip-load Ratio (ρ)	Number of FDD Installations (N_f)	Response Reduction (%)
El Centro	$N = 4$	0.8	1.5	3	58.3
		1.0	1.1	3	55.4
		1.2	0.9	4	51.7
		1.4	0.3	4	67.3
	$N = 6$	1.0	0.3	3	42.7



		1.2	1.7	3	65.6
		1.4	1.5	3	69.0
		1.6	1.1	4	52.6
	$N = 8$	1.2	1.1	4	45.7
		1.4	1.1	5	53.9
		1.6	1.7	6	57.4
		1.8	1.7	7	55.8
	$N = 10$	1.4	0.7	5	40.4
		1.6	0.5	7	48.6
		1.8	1.1	7	61.6
		2.0	0.3	7	62.4
	$N = 12$	1.6	0.5	7	55.7
		1.8	0.5	7	61.3
		2.0	0.5	8	65.0
		2.2	0.5	9	70.8
	$N = 4$	0.8	0.5	3	63.8
		1.0	0.7	3	72.0
		1.2	1.1	4	70.5
		1.4	0.9	4	53.5
	$N = 6$	1.0	0.9	4	71.8
		1.2	1.1	4	66.1
		1.4	0.9	4	57.9
		1.6	1.9	4	65.7
	$N = 8$	1.2	1.9	5	63.9
		1.4	1.1	5	53.9
		1.6	1.7	5	84.4
		1.8	1.3	5	84.3
	$N = 10$	1.4	0.3	5	54.2
		1.6	1.9	5	76.0
		1.8	1.9	7	81.2
		2.0	1.7	7	78.1
	$N = 12$	1.6	0.5	7	73.1
		1.8	1.3	8	71.6
		2.0	1.7	9	75.9
		2.2	0.5	9	74.6
	$N = 4$	0.8	0.7	2	63.7
		1.0	0.7	3	76.7
		1.2	1.1	4	77.3
		1.4	1.1	4	69.5

$N = 6$	1.0	0.7	4	65.9
	1.2	1.7	4	65.7
	1.4	1.1	5	59.8
	1.6	1.5	5	39.1
$N = 8$	1.2	0.7	5	49.1
	1.4	1.9	6	53.4
	1.6	0.3	7	59.2
	1.8	1.3	4	74.8
$N = 10$	1.4	0.5	6	44.9
	1.6	0.5	6	68.6
	1.8	1.5	6	68.9
	2.0	1.9	6	77.6
$N = 12$	1.6	0.9	7	66.9
	1.8	0.9	7	67.4
	2.0	1.7	7	75.9
	2.2	1.7	7	71.5

Values of N_f presented in Table 3 show that optimal number of FDD installations increases or remains constant when fundamental period of the structure increases. As stated before, Lee *et al.* [23] had shown that the optimal values of normalized number of FDD installations (N_f/N) are generally equal to 0.5 in short-period building structures. Accordingly, it is concluded that $(N_f/N)_{opt}$ increases or remains constant in the range of 0.5 through 1 when fundamental period of the structure increases, as shown in Figure (7).

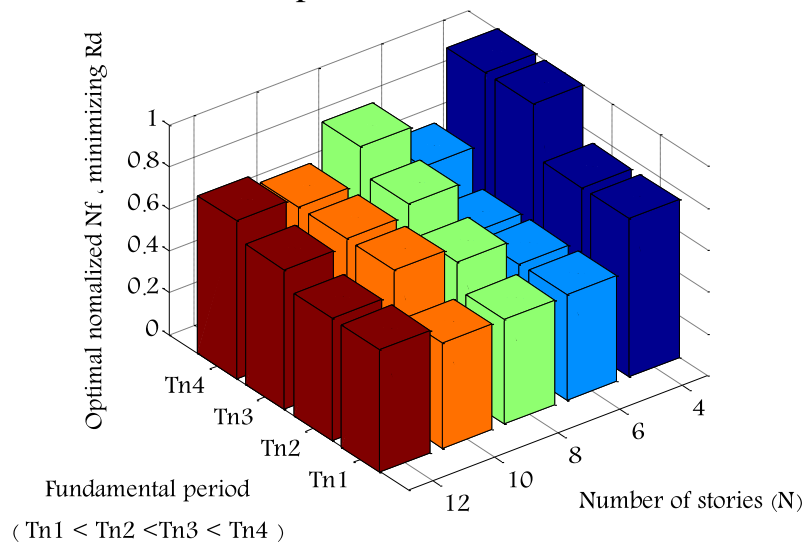


Figure (7): Variations of $(N_f/N)_{opt}$ versus fundamental period of the structures (under excitation of El Centro ground motion typically).

Regarding to results of numerical analyses, optimal configurations of FDD's arrangement along height of the structures do not follow a particular pattern. However, a partial conformity was observed in results of numerical analyses when different FDBS design parameters were assumed. Figure (8) shows probability distributions of FDD installations along height of the structures for different values of N_f . These probability distributions are obtained from comparison of various optimal states of FDD arrangement when other parameters vary. In general, as shown in Figure (8) middle stories have less priority for FDD installation when smaller values of N_f are considered. In accordance with results of numerical analyses, as briefly shown in Table 3, total slip-load ratio (ρ) of the FDD's has a nonlinear influence on dynamic response of the building structures. Consequently, no particular optimality exists for this design parameter of the FDBS and different values of ρ must be checked. However, an optimal range can be considered for ρ minimizing performance index of the structure if another FDBS design parameter, N_f , is well assumed. The results show that variations of the performance index (R_d) are limited to about 10% in the optimal range of ρ . Figure (9) typically shows variations of R_d versus ρ for the 10-storey building model under El Centro ground motion for different fundamental periods when N_f is formerly set equal to its best optimal values. The optimal range of ρ in the example structures of Figure (9) is between 0.5 through 1.5.

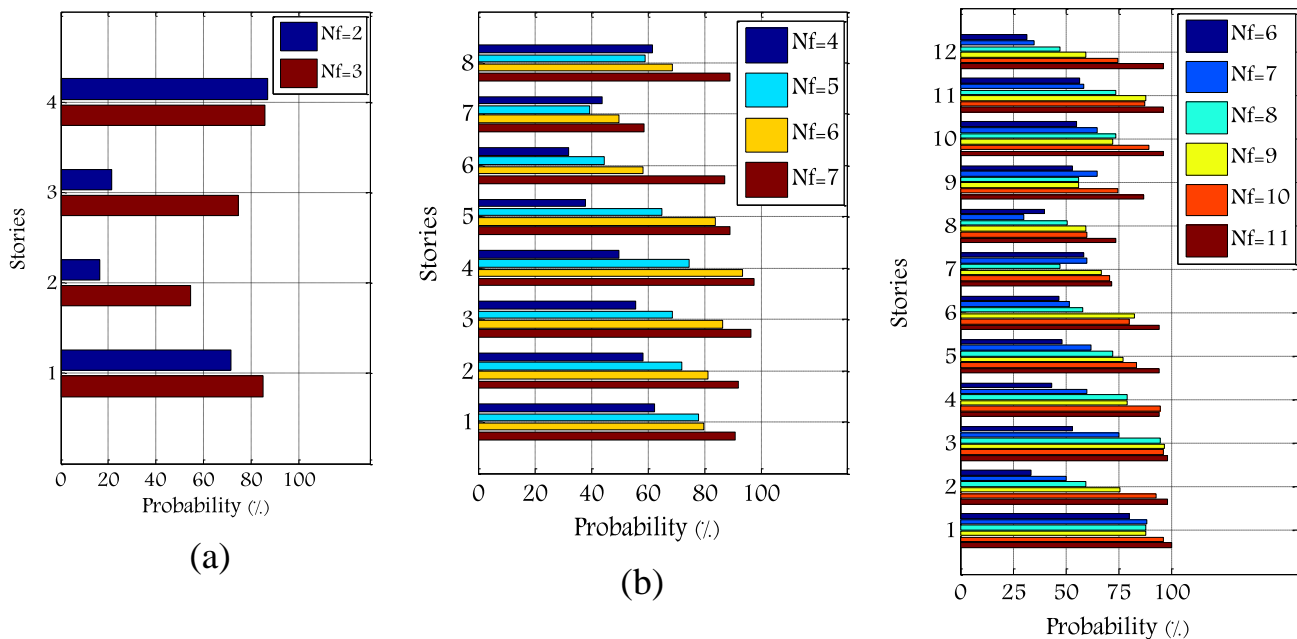


Figure (8): Probability distributions of FDD installations along height of the structures for different values of N_f : (a) 4-storey; (b) 8-storey; (c) 12-storey building structure.

(c)

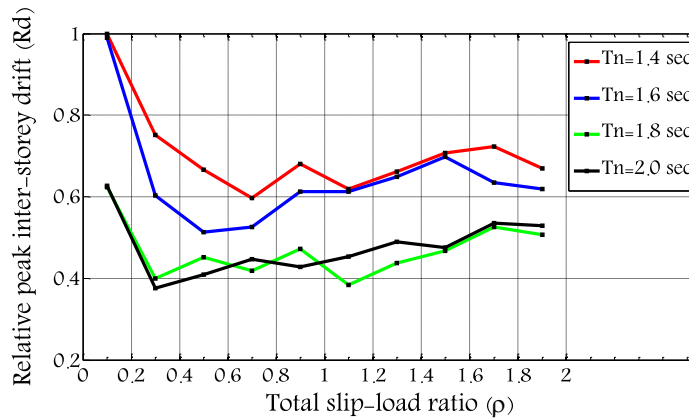


Figure (9): Variations of R_d versus ρ for the 10-storey building model under El Centro ground motion

6. Conclusion:

In this study, influences of FDBS design parameters on seismic performance of low-to-medium multistory building structures are investigated. For this purpose, numerical dynamic model of a SDOF building structure equipped with FDBS is proposed. Design parameters of FDBS in SDOF structures are introduced and their influence on dynamic response of the system is examined. In this procedure, results showed that there is a threshold for stiffness ratio of braces that application of braces with greater stiffness than that no longer mitigates response of the structure significantly. Then, the numerical dynamic model and design parameters of FDBS are generalized to MDOF building structures. In this stage, numerical analyses were performed on some example building models and improvement of seismic response of the structures with respect to variations of design parameters of FDBS including: total slip-load ratio of FDD's, number of FDD installations, and arrangement of dampers along height of building structures, was investigated. In order to examine effects of fundamental period of the structure on design procedure of the FDBS, different periods were considered. Results showed that for a constant stiffness ratio of the braces and uniform distribution of slip-load ratio amongst FDD's, optimal normalized number of FDD installations, $(N_f/N)_{opt}$, increases or remains invariant in the range of 0.5 through 1 when fundamental period of the structure increases. To examine arrangements of FDD installations along height of the structures, different states of damper placement were compared and results showed that no particular optimal pattern exists. However, a partial conformity observed in results of numerical analyses showed that middle stories have less priority for FDD installation when smaller values of N_f are considered. To study influence of total slip-load ratio of FDD's, it was concluded that an optimal range can be considered for ρ minimizing performance index of the structure if another FDBS design parameter, N_f , is well assumed and this optimal range of ρ can be obtained with trial and error.

References:

- [1] A.S. Pall, C. Marsh, Response of friction damped braced frames, *Journal of Structural Engineering* 1982; **108**(9): 1313–23.
- [2] M.C. Constantinou, A. Mokha, A.M. Reinhorn, Teflon bearings in base isolation II: Modeling, *Journal of Structural Engineering* 1990; **116**(2): 455–74.
- [3] C.E. Grigorian, T.S. Yang, E.P. Popov, Slotted bolted connection energy dissipaters, Report of national science foundation, University of California Berkeley, 1992.
- [4] I.H. Mualla, B. Belev, Performance of steel frames with a new friction damper device under earthquake excitation, *Journal of Engineering Structures* 2002; **24**(3): 365–71.
- [5] S.J. Dyke, B.F. Jr Spencer, M.K. Sain, J.D. Carlson, Modeling and control of magnetorheological dampers for seismic response reduction, *Journal of Smart Materials and Structures* 1996; **5**(5): 565–75.
- [6] I.D. Aiken, J.M. Kelly, A.S. Pall, Seismic response of a nine-storey steel frame with friction damped cross-bracing, Ninth World Conference on Earthquake Engineering, Tokyo and Kyoto, Japan, 1988.
- [7] C. Li, A.M. Reinhorn, Experimental and analytical investigation of seismic retrofit of structures with supplemental damping: Part II- Friction devices, Technical report NCEER-95-0009. Buffalo (NY): State University of New York at Buffalo; 1995.
- [8] C.G. Cho, M. Kwon, Development and modeling of a frictional wall damper and its applications in reinforced concrete frame structures, *Journal of Earthquake Engineering and Structural Dynamics* 2004; **33**(7): 821–38.
- [9] J. Marko, D. Thambiratnam, N. Perera, Study of viscoelastic and friction damper configurations in the seismic mitigation of medium-rise structures, *Journal of Mechanics of Materials and Structures* 2006; **1**(6): 1001–39.
- [10] L.Y. Lu, L.L. Chung, L.Y. Wu, G.L. Lin, Dynamic analysis of structures with friction devices using discrete-time state-space formulation, *Journal of Computers and Structures* 2006; **84**: 1049–1071.
- [11] W.I. Liao, I. Mualla, C.H. Loh, Shaking-table test of a friction-damped frame structure, *Journal of the Structural Design of Tall & Special Buildings* 2004; **13**:45–54.
- [12] M.P. Singh, L.M. Moreschi, Optimal seismic response control with dampers, *Journal of Earthquake Engineering and Structural Dynamics* 2001; **30**: 553–572.
- [13] Y.L. Xu, J. Teng, Optimum design of active/passive control devices for tall buildings under earthquake excitation, *Journal of Structural Design of Tall Buildings* 2002; **11**: 109–127.
- [14] J.H. Park, J. Kim, K.W. Min, Optimal design of added viscoelastic dampers and supporting braces, *Journal of Earthquake Engineering and Structural Dynamics* 2004; **33**: 465–484.
- [15] G. Apostolakis, G.F. Dargush, Optimal seismic design of moment-resisting steel

frames with hysteretic passive devices, Journal of Earthquake Engineering and Structural Dynamics 2009; Published online.

[16] R. Levy, O. Lavan, Fully stressed design of passive controllers in framed structures for seismic loadings, Journal of Structural Multidisciplinary Optimization 2006; **32**: 485–498.

[17] W. Pong, Z.H. Lee, C.S. Tsai, B.J. Chen, Heuristic design procedure for structures with displacement-dependent damping devices, Journal of Computer-Aided Engineering and Software 2009; **26**(4): 347–59.

[18] S.K. Lee, J.H. Park, B.W. Moon, K.W. Min, S.H. Lee, J. Kim, Design of a bracing-friction damper system for seismic retrofitting, Journal of Smart Structures and Systems 2008; **4**(5): 685–96.

[19] E. Aydin, M.H. Boduroglu, D. Guney, Optimal damper distribution for seismic rehabilitation of planar building structures, Journal of Engineering Structures 2007; **29**: 176–85.

[20] N. Gluck, A.M. Reinhorn, J. Gluck, R. Levy, Design of supplemental dampers for control of structures, Journal of Structural Engineering 1996; **122**(12): 1394–99.

[21] K. Inoue, S. Kuwahara, Optimum strength ratio of hysteretic damper, Journal of Earthquake Engineering and Structural Dynamics 1998; **27**: 577–88.

[22] D.L. Garcia, T.T. Soong, Efficiency of a simple approach to damper allocation in MDOF structures, Journal of Structural Control 2002; **9**: 19–30.

[23] S.H. Lee, J.H. Park, S.K. Lee, K.W. Min, Allocation and slip load of friction dampers for a seismically excited building structure based on storey shear force distribution, Journal of Engineering Structures 2008; **30**: 930–940.

[24] L.M. Moreschi, M.P. Singh, Design of yielding metallic and friction dampers for optimal seismic performance, Journal of Earthquake Engineering and Structural Dynamics 2003; **32**: 1291–1311.

[25] R. Clough, J. Penzien, Dynamics of Structures, 2nd edition, McGraw-Hill, 1993.

Nomenclatures:

k_f ... lateral stiffness of the frame
 m ... mass of the frame
 c ... damping of the frame
 k_b ... lateral stiffness of brace
 f_s ... slip-load of friction damper
 x ... displacement of frame
 f ... external load
 f_y ... equivalent yield strength
 SR ... stiffness ratio

W ... storey weight
 ρ ... normalized slip-load of FDD
 R_d ... relative peak inter-storey drift
 $x(t)$... inter-storey drift in equipped frame
 $x_0(t)$... inter-storey drift in bare frame
 t ... time
 N_f ... number of FDD installations
 N ... number of stories